(12) INTERNATIONAL APPLICATION PUBLISHED UNDER THE PATENT COOPERATION TREATY (PCT)

(19) World Intellectual Property Organization
International Bureau

(43) International Publication Date
13 October 2011 (13.10.2011)

PCT

(10) International Publication Number
WO 2011/126778 A1

(51) International Patent Classification:
C09K 11/66 (2006.01) *H01L 31/0352* (2006.01)
H01L 31/0296 (2006.01) *H01L 31/072* (2006.01)
H01L 31/032 (2006.01)

(21) International Application Number:
PCT/US2011/030074

(22) International Filing Date:
25 March 2011 (25.03.2011)

(25) Filing Language: English

(26) Publication Language: English

(30) Priority Data:
61/321,450 6 April 2010 (06.04.2010) US
61/334,650 14 May 2010 (14.05.2010) US
12/890,797 27 September 2010 (27.09.2010) US

(71) Applicant *(for all designated States except US)*: **THE GOVERNING COUNCIL OF THE UNIVERSITY OF TORONTO** [CA/CA]; 27 King's College Circle, Toronto, Ontario M5S 1A1 (CA).

(72) Inventors; and
(75) Inventors/Applicants *(for US only)*: **TANG, Jiang** [CN/CA]; 424 Dundas Street West, Toronto, Ontario M5T 1G7 (CA). **PATTANTYUS-ABRAHAM, Andras** [CA/CA]; #607-9298 University Crescent, Burnaby, British Columbia V5A 4X8 (CA). **KRAMER, Illan** [CA/CA]; 505 Northcliffe Blvd., Toronto, Ontario M6E 3L6 (CA). **BARKHOUSE, Aaron** [CA/US]; IBM, T.J. Watson Research Center, P.O. Box 218, Yorktown Heights, New York 10598 (US). **WANG, Xihua** [CN/CA]; 3000 Yonge Street, Apt. 114, Toronto, Ontario M4N 2K5 (CA). **DEBNATH, Ratan** [BD/CA]; University of Toronto, 10 King's College Road, Toronto, Ontario M5S 3G4 (CA). **SARGENT, Edward H.** [CA/CA]; 1 Warren Road, Toronto, Ontario M4V 2R4 (CA). **GERASIMOS, Konstantatos** [GR/ES]; Institute de Ciencies Fotoniques (ICFO), Parc Mediterrani de la Tecnologia, Avda. Canal Olimpic s/n, E-08860 Castelldefels, Barcelona (ES).

(74) Agents: **OSTOMEL, Todd A.** et al.; Kilpatrick Townsend & Stockton LLP, Two Embarcadero Center, Eighth Floor, San Francisco, California 94111-3834 (US).

(81) Designated States *(unless otherwise indicated, for every kind of national protection available)*: AE, AG, AL, AM, AO, AT, AU, AZ, BA, BB, BG, BH, BR, BW, BY, BZ, CA, CH, CL, CN, CO, CR, CU, CZ, DE, DK, DM, DO, DZ, EC, EE, EG, ES, FI, GB, GD, GE, GH, GM, GT, HN, HR, HU, ID, IL, IN, IS, JP, KE, KG, KM, KN, KP, KR, KZ, LA, LC, LK, LR, LS, LT, LU, LY, MA, MD, ME, MG, MK, MN, MW, MX, MY, MZ, NA, NG, NI, NO, NZ, OM, PE, PG, PH, PL, PT, RO, RS, RU, SC, SD,

[Continued on next page]

(54) Title: PHOTOVOLTAIC DEVICES WITH DEPLETED HETEROJUNCTIONS AND SHELL-PASSIVATED NANOPARTICLES

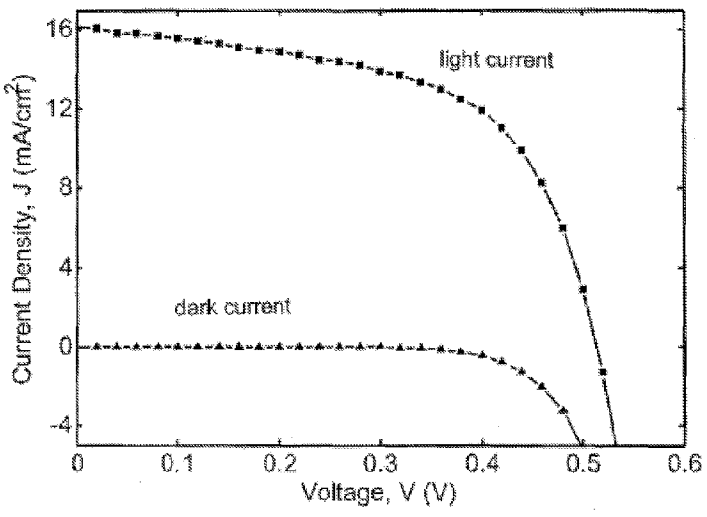

FIG. 1

(57) Abstract: Photovoltaic cells are fabricated in which the compositions of the light-absorbing layer and the electron-accepting layer are selected such that at least one side of the junction between these two layers is substantially depleted of charge carriers, i.e., both free electrons and free holes, in the absence of solar illumination. In further aspects of the invention, the light-absorbing layer is comprised of dual-shell passivated quantum dots, each having a quantum dot core with surface anions, an inner shell containing cations to passivate the core surface anions, and an outer shell to passivate the inner shell anions and anions on the core surface.

WO 2011/126778 A1

SE, SG, SK, SL, SM, ST, SV, SY, TH, TJ, TM, TN, TR, TT, TZ, UA, UG, US, UZ, VC, VN, ZA, ZM, ZW.

(84) Designated States *(unless otherwise indicated, for every kind of regional protection available)*: ARIPO (BW, GH, GM, KE, LR, LS, MW, MZ, NA, SD, SL, SZ, TZ, UG, ZM, ZW), Eurasian (AM, AZ, BY, KG, KZ, MD, RU, TJ, TM), European (AL, AT, BE, BG, CH, CY, CZ, DE, DK, EE, ES, FI, FR, GB, GR, HR, HU, IE, IS, IT, LT, LU, LV, MC, MK, MT, NL, NO, PL, PT, RO, RS, SE, SI, SK, SM, TR), OAPI (BF, BJ, CF, CG, CI, CM, GA, GN, GQ, GW, ML, MR, NE, SN, TD, TG).

Published:

— *with international search report (Art. 21(3))*

PHOTOVOLTAIC DEVICES WITH DEPLETED HETEROJUNCTIONS AND SHELL-PASSIVATED NANOPARTICLES

CROSS-REFERENCES TO RELATED APPLICATIONS

[0001] This patent application claims the benefit of U.S. Patent Application No. 12/890,797, filed September 27, 2010, which claims the benefit of United States Provisional Patent Application No. 61/334,650, filed May 14, 2010, and United States Provisional Patent Application No. 61/321,450, filed April 6, 2010, the contents of which are hereby incorporated herein by reference in their entirety.

BACKGROUND OF THE INVENTION

1. Field of the Invention

[0002] This invention resides in the fields of photovoltaic cells and quantum dots.

2. Description of the Prior Art

[0003] Solar cells that generate electricity through the photovoltaic effect require a combination of low cost and high efficiency in order for such cells to offer a practical alternative to traditional means of power generation. One way in which the cost of manufacturing a photovoltaic cell can be lowered is by the use of solution processing to form the layer of light-harvesting material that is part of the cell. The efficiency of the cell, however, depends on the cell materials, including the light-harvesting material. The optimal light-harvesting material is one that achieves a high short-circuit current density J_{sc} by maximizing the absorption of the sun's rays in both the visible and infrared spectra, and that one extracts a high level of work, in the form of a high open-circuit voltage V_{oc} and a high fill factor FF, from each absorbed photon. For an input solar intensity P_{solar} (typically 100 mW cm^{-2}), the power conversion efficiency η is defined as

$$\eta = \frac{V_{oc} J_{sc} FF}{P_{solar}}$$

[0004] It has been reported by Sargent, E., in "Infrared photovoltaics made by solution processing," *Nat. Photonics* **3**, 325-331 (2009), and Hillhouse H.S., *et al.*, in "Solar cells

from colloidal nanocrystals: Fundamentals, materials, devices, and economics" *Curr. Opin. Colloid Interface Sci.* **14**, 245-259 (2009), that the use of colloidal quantum dots as the light-harvesting material provides photovoltaic cells with high power conversion efficiencies. Colloidal quantum dot photovoltaics offer both the ability to form the light-harvesting layer by solution processing and the ability to tune the bandgap over a wide range, benefits that are available in both single-junction and multijunction cells. The ability to tune the bandgap also enables the use of inexpensive, abundant ultralow-bandgap semiconductors that are otherwise unsuitable for photovoltaic energy conversion. By combining lead chalcogenide quantum dots and Schottky junctions, photovoltaic cells with efficiencies of 3.4% have been achieved, as reported by Ma, W., *et al.*, "Photovoltaic devices employing ternary PbS_xSe_{1-x} Nanocrystals," *Nano Lett.* **9**, 1699-1703 (2009), and others. Significant progress has also been achieved by sensitizing nanoporous TiO_2 electrodes with a thin layer of colloidal quantum dots, with power conversion efficiencies of 3.2%. See for example Fan, S., *et al.*, "Highly efficient CdSe quantum-dot-sensitized TiO_2 photoelectrodes for solar cell applications," *Electrochem. Commun.* **11**, 1337-1330 (2009).

[0005] Both colloidal quantum dots and Schottky devices pose certain limitations photovoltaic efficiencies, however. In Schottky devices, both the V_{oc} and the *FF* values have fallen well below their potential, and in cells sensitized by colloidal quantum dots, the J_{sc} values are generally lower despite the increases in V_{oc} and *FF*.

SUMMARY OF THE INVENTION

[0006] It has now been discovered that the limitations of colloidal quantum dot photovoltaics as noted above can be significantly reduced or overcome by the pairing of a layer of light-harvesting nanoparticles with a layer of an electron-accepting material such that the junction between these layers is substantially depleted of both free electrons and free holes on at least one side of the junction when the device is not illuminated. An effective means of achieving this depletion is by selecting materials for these two layers that are of different bandgap magnitudes. Such a junction is thus a heterojunction by virtue of the two different materials on either side of the junction, and in particular a depleted heterojunction by virtue the low level or absence of both free electrons and free holes in the vicinity of the junction. The depletion arises from charge transfer from the electron-accepting contact to the to the nanoparticles. In certain embodiments of the invention, the nanoparticles are quantum dots, include p-type colloidal quantum dots, and the electron-accepting layer is, or includes, a metal oxide. The depletion is at least partly attributable to a relatively low charge density in

the electron-accepting layer, as compared to that of the metal contact of a Schottky junction, which has a very high free electron density.

[0007] Particular embodiments of photovoltaic devices within the scope of this invention offer further advantages over photovoltaic devices of the prior art. For example, the use of a metal oxide as the electron-accepting layer allows the device to be configured with the electron-accepting layer as the front surface of the device or as the layer that the solar rays first penetrate upon entering the two semiconductor layers that form the photovoltaic junction. The electrons liberated by the rays are thus less susceptible to recombination with the holes since the electrons in these embodiments have a shorter distance to travel before reaching their destination electrode. Also, in embodiments in which the junction is that between a metal oxide and quantum dots, the junction is better defined and easier to passivate, and thus less susceptible to defects, than a metal-semiconductor Schottky junction. This avoids the occurrence of Fermi-level pinning at the interface. Still further, these embodiments present less of a barrier to hole injection than a Schottky device by introducing a large discontinuity in the valence band and by minimizing the electron density at the interface.

[0008] It has further been discovered that the performance of nanocrystals in photovoltaic devices and in optoelectronic devices in general, and particularly nanocrystals with surface anions, is enhanced by depositing cations over the nanocrystals to form a first or inner shell and deposing anions over the first shell to form a second or outer shell. The inner and outer shells together passivate surface defects on the nanocrystal which tend to disrupt the quantum confinement of the nanocrystal. Passivation is known to be achievable by the placement of short organic ligands such as ethanedithiol, butylamine, or mercaptopropionic acid on the nanocrystal surface. The use of cation and anion shells in place of these ligands offers the advantages that the cation shells bind to the anions on the nanocrystal surface rather than to the cations, as organic ligands tend to do, and the ionic bonds are stable upon exposure to air and light, and particularly moisture, oxygen, and heat. Further advantages of these cation and anion shells are that by avoiding the need for organic ligands, these shells allow the nanocrystals to reside very close to each other in the light-absorbing film and thereby promote electron wave function overlap and carrier mobility, valuable features that are typically impeded by organic ligands.

BRIEF DESCRIPTION OF THE FIGURES

[0009] FIG. **1** is a plot of current density *vs.* voltage for examples of depleted heterojunction photovoltaic cells within the scope of the present invention.

[0010] FIG. **2** is a plot of current *vs.* voltage for examples of depleted heterojunction photovoltaic cells within the scope of the present invention.

[0011] FIG. **3** is a plot of external quantum efficiency *vs.* wavelength for examples of depleted heterojunction photovoltaic cells within the scope of the present invention.

[0012] FIG. **4** is a plot of device capacitance *vs.* bias voltage and device resistance *vs.* bias voltage for examples of depleted heterojunction photovoltaic cells within the scope of the present invention.

[0013] FIG. **5** shows absorption spectra of examples of depleted heterojunction photovoltaic cells with dual-shell-passivated quantum dots within the scope of the present invention.

[0014] FIG. **6** is a plot of carrier lifetime *vs.* light intensity for examples of depleted heterojunction photovoltaic cells with dual-shell-passivated quantum dots within the scope of the present invention.

[0015] FIG. **7** is a plot of current density *vs.* voltage for examples of depleted heterojunction photovoltaic cells with dual-shell-passivated quantum dots within the scope of the present invention.

DETAILED DESCRIPTION OF ILLUSTRATIVE EMBODIMENTS OF THE INVENTION

[0016] The term "substantially depleted" as used herein to characterize the region(s) adjacent to a heterojunction denotes that the charge density in the region(s) is orders of magnitude less than that of the metal side of a Schottky junction. In certain heterojunction regions of the invention, the charge density is three or more orders of magnitude less than the charge density of conducting metals, and in many of these, the charge density is four or more, five or more, or six or more orders of magnitude less. Particularly effective results can be achieved when the depleted charge density is on the n-type electron accepting layer side of the junction. In many embodiments of the invention, a range of charge density in the depleted region is about 1×10^{12} cm^{-1} to about 1×10^{18} cm^{-1}, or alternatively about 1×10^{14}

cm^{-1} to about 1×10^{17} cm^{-1}, or as a further alternative about 1×10^{15} cm^{-1} to about 1×10^{16} cm^{-1}.

[0017] To achieve a depleted heterojunction by use of materials of different bandgap magnitudes on the two sides of the junction, effective results in many cases can be achieved with a bandgap difference (*i.e.*, the difference between the bandgap magnitude on one side of the junction and the bandgap magnitude on the other side of the junction) of at least about 1.5eV, or within the range of from about 1.5eV to about 5eV, or even more effectively within the range of from about 2eV to about 5eV. With an n-type electron-accepting layer on one side of the junction and p-type light-absorbing nanoparticles on the other, the bandgap of greater magnitude will reside in the n-type electron-accepting layer.

[0018] Quantum dots are particularly useful as the nanoparticles, and colloidal quantum dots, *i.e.*, quantum dots manufactured by colloid chemistry, are notable examples. Of these, metal chalcogenide quantum dots are well known in the art, and lead chalcogenide, and particularly lead sulfide, quantum dots are of particular interest. Quantum dots are known to absorb light at wavelengths related to the diameters of individual quantum dots, and this property can be used in the present invention to select or optimize the light-absorbing characteristics of the quantum dots. In many cases, quantum dots with a number-average diameter within the range of about 2nm to about 15nm can be used effectively, while those with a number-average diameter within the range of about 3nm to about 10nm are often the most appropriate, and among these the range of about 3nm to about 6nm are often even more useful.

[0019] The n-type electron-accepting layer can vary widely in composition, provided that the combination of n-type electron-accepting layer and light-absorbing nanoparticles when placed in contact form the depleted heterojunction described above. Metal oxides are examples of materials that can serve effectively as the n-type electron-accepting layer, and a particularly useful example of a metal oxide is titanium dioxide.

[0020] In those aspects of the invention that relate to nanoparticles with inner passivating shells of cations and outer passivating shells of anions, the core of such a nanoparticle is generally a quantum dot having exposed anions at its surface. As noted above, the quantum dot core is in many cases a metal chalcogenide colloidal quantum dot, most often a metal sulfide colloidal quantum dot. A noted example is lead sulfide, and lead sulfide quantum dots are often lead rich, with a surface composed primarily of exposed Pb^{2+} ions but also containing exposed S^{2-} ions. The cations of the inner shell bind to, and thereby passivate, the

S^{2-} ions at the core surface, while the anions in the outer shell bind to, and thereby passivate, the cations of the inner shell. Examples of cations that can be used for the first shell are Cd^{2-}, Pb^{2+}, Zn^{2+}, and Sn^{2+}. Among these, Cd^{2+} is particularly convenient and effective. Examples of anions effective for use as the second shell are halogen ions and the thiocyanate ion. Of these, halogen ions, and particularly bromine ion, are optimal or particularly convenient in certain cases. These dual-shelled nanoparticles are useful as the light-absorbing nanoparticles of the depleted heterojunctions described above, but are also useful in optoelectronic devices in general, *i.e.*, any devices in which the particles serve to absorb light energy and convert the absorbed energy to an electric current.

[0021] In further aspects, therefore, the present invention resides in the formation of passivated p-type semiconductor nanoparticles without using organic ligands as passivating agents. This is achieved by treating p-type semiconductor quantum dots that have surface anions with a solution of a cation-containing reagent that passivates the surface anions, and then treating the resulting cation-treated quantum dot core with a solution of a reagent that contains anions that passivate the cations. Noting the example of Cd^{2+} as a cation useful for the passivation of the quantum dot core, an example of a Cd^{2+}-containing reagent is cadmium(II) chloride-tetradecylphosphonic acid-oleylamine. Examples of anion-containing reagents are quaternary ammonium halides and thiocyanates, and specific examples are cetyltrimethylammonium bromide, hexatrimethylammonium chloride, tetrabutylammonium iodide, and tetrbutylammonium thiocyanate.

[0022] Photovoltaic devices utilizing one or more of the features described above will typically contain at least two electrodes, one electrically connected to each of the two semiconductor layers of the heterojunction. In a heterojunction between a n-type metal oxide layer and a layer of p-type metal chalcogenide colloidal quantum dots, for example, a first electrode will be in direct electrical contact with the n-type metal oxide layer and a second electrode will be in contact with the colloidal quantum dot layer. The first electrode in many cases is a light-transmitting electrode, and examples are aluminum oxide, zinc oxide, indium tin oxide (ITO), and fluorine-doped tin oxide (FTO). The second electrode in many cases is either nickel, lithium fluoride, platinum, palladium, silver, gold, or copper, or alloys of two or more of these metals, such as alloys of silver, gold, and copper. One example of a combination of electrode materials is fluorine-doped tin oxide as the first electrode and gold as the second electrode.

EXAMPLE 1

[0023] This example illustrates the preparation of depleted heterojunction photovoltaic cells within the scope of the present invention, each formed by depositing a layer of PbS colloidal quantum dots (approximately 10^{17} cm^{-3} n-type doping) of varying diameters -- 3.7nm (bandgap 1.3eV), 4.3nm (bandgap 1.1eV), and 5.5nm (bandgap 0.9eV) -- over transparent TiO_2 electrodes.

[0024] The TiO_2 electrodes were prepared on SnO_2:F (FTO)-coated glass substrates (Pilkington TEC 15, Hartford Glass, Inc., Hartford City, Indiana, USA) with a TiO_2 paste (DSL-90T, Dyesol Ltd., Queanbeyan, NSW, Australia) as follows. The FTO substrates were first rinsed with toluene, then sonicated for twenty minutes in a mixture of Triton in de-ionized water (1-3% by volume). Separately, a TiO_2 paste was prepared by combining one part by weight TiO_2 nanoparticles with three parts by weight terpineol. The paste was then spin cast at 1500rpm for ninety seconds on the $TiCl_4$-treated FTO substrates. One edge of each substrate was then wiped free of the paste with a swab soaked in isopropyl alcohol to expose a section of claim FTO for electrical contacting. This was immediately followed by sintering for one hour on a hotplate at 400°C. The substrates were then placed in a bath of 60mM $TiCl_4$ in de-ionized water, and baked in the bath at 70°C for thirty minutes. They were then rinsed with de-ionized water, dried with nitrogen, and placed in a 520°C tube furnace for one hour, then cooled to room temperature. The sample was then allowed to cool, and the $TiCl_4$ treatment was repeated, followed by a final heating to 520°C. The substrates were then placed in individual substrate holders and stored in air for up to one week prior to further processing.

[0025] PbS colloidal quantum dots were prepared as follows. Bis(trimethylsilyl)sulphide (TMS, synthesis grade) (0.18g, 1mol) was added to 1-octadecene (10mL), which had been dried and degassed by heating to 80°C under vacuum for 24 hours. A mixture of oleic acid (1.34g, 4.8mmol), PbO (0.45g, 2.0mmol), and 1-octadecene (14.2g, 56.2mmol) was heated to 95°C under vacuum for sixteen hours, then placed under Ar. The flask temperature was increased to 120°C and the TMS/octadecene mixture was injected, causing the temperature to drop to about 95°C, and the flask was allowed to cool to 36°C. The nanocrystals were precipitated with 50mL of distilled acetone and centrifuged under ambient conditions. The supernatant was then discarded, and the precipitate was redispersed in toluene, precipitated again with 20mL of acetone, centrifuged for five minutes, dried, and again dispersed in toluene (about 200mg mL^{-1}). The nanocrystals were then placed in a N_2-filled glove box,

where they were precipitated twice with methanc and then finally redispersed at 25 or 50mg mL^{-1} in octane.

[0026] The resulting oleate-capped PbS quantum dots were deposited on the TiO_2 by multilayer spin-coating of the TiO_2 surface with 25 or 50 mg/mL solutions of the quantum dots in octane under ambient conditions. Each layer was deposited at 2500 rpm, then treated briefly with 10% 3-mercaptopropionic acid in methanol to displace the oleate ligand and thereby render the quantum dots insoluble, then rinsed with methanol and octane. Fifteen deposition cycles using the 25mg/mL dispersion produced thermally stable layers 22nm in thickness on the TiO_2 substrate, and eight deposition cycles using the 50mg/mL dispersion also produced thermally stable layers of the same thickness. Each layered medium was then transferred to a glove box with N_2 atmosphere and left overnight. A gold contact was then deposited on the quantum dot layer by DC sputtering with 5mTorr Ar pressure at a power density of 1 W cm^{-2} through a shadow mask to thicknesses of 150nm to 200nm. Spatially-resolved X-ray elemental analyses and transmission electron microscopy were performed on a thin section sample prepared by focused-ion-beam milling, and revealed very little interpenetration of the quantum dot and TiO_2 layers.

[0027] FIG. **1** is a plot of the photovoltaic response of a depleted heterojunction solar cell as prepared above, expressed as current density in mA cm^{-2} *vs.* voltage, with the lower curve representing the dark current and the upper curve representing the illuminated current of a cell fabricated with 1.3eV-bandgap quantum dots (3.7nm). The data was measured using a Keithley 2400 source-meter under ambient conditions. The solar spectrum at AM1.5 was simulated to within class A specifications with a Xe lamp and filters with the intensity adjusted to 100mW cm^{-2}. The source intensity was measured with a Melles-Griot broadband power meter (responsive from 300nm to 2000nm), through a circular 0.049cm^2 aperture at the position of the sample and confirmed with a calibrated solar cell. The accuracy of the power measurement was estimated to be ±7%. For the five devices having 1.3eV-bandgap quantum dots, the average value of V_{oc} was 0.53 ± 0.02V, the average value of J_{sc} was 15.4 ± 1.4mA cm^{-2}, and the average value of *FF* was 57 ± 4%. The average AM1.5 power conversion efficiency η was thus 4.9 ± 0.3%. For the highest-performing device, V_{oc} was 0.52V, J_{sc} was 16.4mA cm^{-2}, and *FF* was 58%, yielding η of 5.1%.

[0028] FIG. **2** is a plot of the photovoltaic response of a depleted heterojunction solar cell as prepared above, expressed as current in mA *vs.* voltage, with the lower curve representing cells fabricated with 0.9eV-bandgap (5.5nm) quantum dots, the middle curve representing the cells fabricated with 1.1eV-bandgap (4.3nm) quantum dots, and the upper curve representing

the cells fabricated with 1.3eV-bandgap (3.7nm) quantum dots. This figure shows that the largest quantum dots had the smallest driving force for electron transfer in TiO_2, and yet devices with these 0.9eV bandgaps still showed a short-circuit current density J_{sc} above 10mA/cm^2 and an open-circuit voltage V_{oc} of 0.38V. This indicates that minimal band offset is required for efficient electron transfer from the PbS colloidal quantum dots into the TiO_2 electrode. This is in contrast to organic photovoltaics, which have a large band offset between the electron donor and acceptor, the large band offset imposing a substantial penalty on efficiency.

[0029] FIG. **3** is a plot of external quantum efficiency (EQE) *vs.* wavelength and of absorption *vs.* wavelength, with the lower curve representing the EQE for the best-performing 1.3eV-bandgap quantum dot device and the upper curve representing the spectral absorption of the same device. The EQE is the ratio of extracted electrons to incident photons and the curve is also known as the incident photon conversion efficiency spectrum. The EQE was obtained by passing the output of a 400W Xe lamp through a monochromator and using appropriate order-sorting filters. The collimated output of the monochromator was measured through a 1.5nm aperture with a calibrated Newport 818-UV power meter. The measurement bandwidth was about 40nm and the intensity varied with the spectrum of the Xe lamp. The average intensity was 0.3mW cm^{-2}. The current-voltage response was measured with Keithley 2400 source-meters. The plot shows that at short wavelengths, the EQE reached values above 60%, while at longer wavelengths the EQE had a peak of 24%.

[0030] FIG. **4** is a plot of device capacitance *vs.* bias voltage and of device resistance *vs.* bias voltage. The capacitance arises from the depletion layer due to charge transfer from TiO_2 to the PbS colloidal quantum dot layer. Capacitance-voltage measurements were performed directly on the photovoltaic devices using an Agilent 4284A LCR meter. Absorption spectroscopy was performed on a Cary 500 UV-vis-IR Scan photospectrometer. The impedance was acquired at 2kHz with a signal amplitude of 10mV, and is represented in FIG. **4** in terms of equivalent parallel resistance R_p and capacitance C_p for a device with a contact area of 0.03cm^3. The plot shows that the capacitance, and its associated depletion layer distributed between the two semiconductors, persist up to a bias of 0.6V, close to the observed open-circuit voltage value. This is a direct indication of the presence of a built-in field that efficiently drives the separation of photogenerated carriers.

EXAMPLE 2

[0031] This example illustrates the preparation and use of nanoparticles containing a quantum dot core, an inner shell of cations and an outer shell of anions, within the scope of the present invention.

[0032] Colloidal quantum dots capped with oleic acid ligands were synthesized and stripped of their oleate ligands, in the manner described in Example 1. These quantum dots were prepared with an excess of Pb during synthesis, resulting in a lead-rich bulk composition but with sulfur atoms on their surfaces, either from nonpolar {100} and {110} or polar {111} facets in their crystal structure. To form the inner shell of Cd cations over these PbS cores, the nanoparticles were treated with a solution of $CdCl_2$-tetradecylphosphonic acid-oleylamine ($CdCl_2$-TDPA-OLA). This treatment resulted in a slight redshift (between 6 and 24nm) of the excitonic absorption, suggesting growth of a partial monolayer of highly cation-rich material on the surface, an interpretation reinforced by the approximately 30nm blueshift observed when a control treatment involving TDPA-OLA only (no $CdCl_2$) was implemented. Elemental analysis and X-ray photoelectron microscopy both indicated 0.3% atomic ratio of cadmium to other elements present in powders of the resultant samples. X-ray diffraction indicated that no purely Cd-based phase (such as CdS) was present.

[0033] An outer shell of bromine ions was then applied by the use of a solution of cetyltrimethylammonium bromide in methanol. The cetyltrimethylammonium cations combined with any remaining oleates on the particles to form salts that were then removed with a final methanol rinse. The cetyltrimethylammonium bromide treatment and methanol rinse were conducted in air at room temperature (23°C), including the absence of hydrazine. The absence of any appreciable amounts of organics at the outer surfaces of the treated particles was confirmed by FTIR spectra showing a complete absence of C-H vibrations at $2922cm^{-1}$ and $2852cm^{-1}$. The presence of a significant amount of bromide in the outer applied film was confirmed by X-ray photoelectron spectroscopy (XPS) and energy-dispersive X-ray spectroscopy (EDX), and simple calculation indicated an approximate 1:1 ratio of bromide ions to surface cations. Elemental analysis confirmed that the 0.3% of Cd cations present following the initial $CdCl_2$-TDPA-OLA were still present after application of the bromide shell.

[0034] Photovoltaic devices utilizing these dual-shell-passivated quantum dots were fabricated in the same manner as described in Example 1 above. A scanning electron micrograph showed that the quantum dot layer was approximately 300nm in thickness and

was free of the voids and cracks that often occur in films made from layer-by-layer deposition. Absorption spectra of the devices were obtained in a double pass by including reflection from the Au top contact. The spectra of devices made using 9, 11, and 13 quantum dot layers are shown in FIG. **5**, which also includes corresponding spectra from the bare FTO/TiO_2 substrate. The absorption peak at 950nm is the excitonic peak of the PbS quantum dots. This indicates that quantum confinement of the core quantum dots was preserved in the shelled form. A reduction in interparticle distance is suggested by the red-shift (~100meV) of the excitonic peak in the final film as compared to the excitonic peak of dots in solution. Upon exposure to 100 mW/cm^2 solar illumination, the device showed an open circuit voltage (V_{oc}) of 0.45V, a short-circuit current density (J_{sc}) of 21.8mA/cm^2, and a fill factor (*FF*) of 59%, yielding a power conversion efficiency η of 5.76%. Integration of the net absorption of the quantum dot film over the AM1.5G spectrum indicates that a film having 100% quantum efficiency would have achieved a circuit current density (J_{sc}) of 24.4mA/cm^2. Comparing this with the measured circuit current density (J_{sc}) of 21.8mA/cm^2 indicates that the internal quantum efficiency (IQE) averaged across the entire broadband absorbing region of 400-1150nm exceeds 90%, indicating minimal recombination loss and efficient carrier extraction.

[0035] The doping density and carrier lifetime of the dual-shell-passivated quantum dot films were determined by capacitance-voltage (C-V) and V_{oc} decay analyses, respectively. The C-V analysis showed that doping was a full order of magnitude lower than in the lowest-doped organic ligand PbS and PbSe quantum dot films, and the carrier lifetime τ, which is shown in FIG. **6**, was approximately twice as long as that of a control device made using a bidentate organic ligand (3-mercaptopropionic acid, also shown in FIG. **6**), reaching a remarkably long lifetime of over 40 μsec even under full solar 100 mW/cm^2 illumination.

[0036] The dual-shell-passivated quantum dots also demonstrated an improved resistance to oxidation. FIG. **7** is a plot of current density *vs.* voltage, comparing a layer of dual-shell-passivated quantum dots in accordance with the invention with quantum dots bearing 3-mercaptopropionic acid ligands, each shown both fresh (immediately after fabrication) and after ten days of storage under ambient conditions on a laboratory bench. The dual-shell-passivated quantum dots showed no significant change in performance over the ten-day period, while the organic ligand-capped quantum dots underwent a complete loss of efficiency over the same period.

[0037] To demonstrate the effectiveness of inner shells of anions other than bromide ions, devices were made containing dual-shell-passivated quantum dots with a variety of anions, and measurements of the photovoltaic performance characteristics were made. The anion-

bearing reagents were hexatrimethylammonium chloride (HTAC), cetyltrimethylammonium bromide (CTAB), tetrabutylammonium iodide (TBAI), and tetrabutylammonium thiocyanate (TBAT). The parameters measured were J_{sc} in mA/cm^2, V_{oc} in V, FF in %, η in %, shunt resistance R_{sh} and series resistance R_s, and rectification (the current between forward bias +1V and reverse bias -1V), and are listed in the following Table.

Reagent	Ligand	J_{sc}	V_{oc}	FF	η	R_{sh}	R_s	Rectification
HTAC	Cl^-	17.1	0.43	55%	4.08%	3388	1112	10391
CTAB	Br^-	21.8	0.35	59%	5.76%	3351	60	2920
TBAI	I^-	20.2	0.43	43%	3,76%	3195	148	4916
TBAT	SCN^-	13.9	0.43	30%	1.72%	1924	847	4232

[0038] In the claims appended hereto, the term "a" or "an" is intended to mean "one or more." The term "comprise" and variations thereof such as "comprises" and "comprising," when preceding the recitation of a step or an element, are intended to mean that the addition of further steps or elements is optional and not excluded. All patents, patent applications, and other published reference materials cited in this specification are hereby incorporated herein by reference in their entirety. Any discrepancy between any reference material cited herein or any prior art in general and an explicit teaching of this specification is intended to be resolved in favor of the teaching in this specification. This includes any discrepancy between an art-understood definition of a word or phrase and a definition explicitly provided in this specification of the same word or phrase.

WHAT IS CLAIMED IS:

1. A photoelectric device comprising:

a light-transmitting first electrode,

a first semiconductor layer in direct electrical contact with said first electrode,

a second semiconductor layer in direct electrical contact with said first semiconductor layer and comprising light-absorbing nanoparticles, and

a second electrode in direct electrical contact with said second semiconductor layer,

said first and second semiconductor layers forming a junction therebetween, at least one side of which is substantially depleted of free electrons and of free holes when said device is not illuminated.

2. The photoelectric device of claim **1** wherein said first semiconductor layer is an n-type electron-accepting layer, and said light-absorbing nanoparticles of said second semiconductor layer are p-type nanoparticles, wherein said n-type electron-accepting layer and said p-type nanoparticles have bandgaps of sufficiently different magnitudes to cause said at least one side of said junction to be so depleted.

3. The photoelectric device of claim **2** wherein said bandgap of said n-type electron-accepting layer is greater than said bandgap of said layer of p-type light-absorbing nanoparticles by at least about 1.5eV.

4. The photoelectric device of claim **2** wherein said bandgap of said n-type electron-accepting layer is greater than said bandgap of said layer of p-type light-absorbing nanoparticles by from about 1.5eV to about 5eV.

5. The photoelectric device of claim **2** wherein said bandgap of said n-type electron-accepting layer is greater than said bandgap of said layer of p-type light-absorbing nanoparticles by from about 2eV to about 5eV.

6. The photoelectric device of claim **1** wherein said p-type light-absorbing nanoparticles are colloidal quantum dots.

7. The photoelectric device of claim **1** wherein said p-type light-absorbing nanoparticles are metal chalcogenide colloidal quantum dots.

8. The photoelectric device of claim **1** wherein said p-type light-absorbing nanoparticles are lead chalcogenide colloidal quantum dots. .

9. The photoelectric device of claim **1** wherein said p-type light-absorbing nanoparticles are lead sulfide colloidal quantum dots.

10. The photoelectric device of claim **6** wherein said colloidal quantum dots have a number-average diameter of from 3nm to 6nm.

11. The photoelectric device of claim **1** wherein said light-absorbing nanoparticles are nanoparticles comprising a quantum dot core having a surface comprising anions at said surface, a first shell surrounding said quantum dot core and comprising cations that passivate said anions at said core surface, and a second shell surrounding said first shell and comprising anions that passivate any cations present at said core surface and said cations of said first shell.

12. The photoelectric device of claim **11** wherein said quantum dot core is a metal chalcogenide colloidal quantum dot.

13. The photoelectric device of claim **11** wherein said quantum dot core is a metal sulfide colloidal quantum dot.

14. The photoelectric device of claim **11** wherein said quantum dot core is a metal sulfide colloidal quantum dot and said cations of said first shell are a member selected from the group consisting of Cd^{2+}, Pb^{2+}, Zn^{2+}, and Sn^{2+}.

15. The photoelectric device of claim **11** wherein said quantum dot core is a metal sulfide colloidal quantum dot and said cations of said first shell are Cd^{2-}.

16. The photoelectric device of claim **11** wherein said cations of said first shell are Cd^{2+} and said anions of said second shell are a member selected from the group consisting of halogen ions and thiocyanate ion.

17. The photoelectric device of claim **11** wherein said quantum dot core is a metal sulfide colloidal quantum dot, said cations of said first shell are Cd^{2+}, and said anions of said second shell are halogen ions.

18. The photoelectric device of claim **11** wherein said quantum dot core is a metal sulfide colloidal quantum dot, said cations of said first shell are Cd^{2+}, and said anions of said second shell are bromine ions.

19. The photoelectric device of claim **2** wherein said n-type electron-accepting layer is titanium dioxide.

20. The photoelectric device of claim **1** wherein said light-transmitting first electrode is a member selected from the group consisting of aluminum oxide, zinc oxide, indium tin oxide, and fluorine-doped tin oxide.

21. The photoelectric device of claim **1** wherein said light-transmitting first electrode is fluorine-doped tin oxide.

22. The photoelectric device of claim **1** wherein said second electrode is a member selected from the group consisting of nickel, lithium fluoride, platinum, palladium, silver, gold, copper, and alloys of silver, gold, and copper.

23. The photoelectric device of claim **1** wherein said second electrode is gold.

24. A nanoparticle comprising:

a quantum dot core;

a first shell comprising cations that substantially completely surround said quantum dot core; and

a second shell comprising anions that substantially completely surround said first shell.

25. The nanoparticle of claim **24** wherein said quantum dot core is a metal chalcogenide colloidal quantum dot.

26. The nanoparticle of claim **24** wherein said quantum dot core is a metal sulfide colloidal quantum dot.

27. The nanoparticle of claim **24** wherein said quantum dot core is a metal sulfide colloidal quantum dot and said cations of said first shell are a member selected from the group consisting of Cd^{2+}, Pb^{2+}, Zn^{2+}, and Sn^{2+}.

28. The nanoparticle of claim **24** wherein said quantum dot core is a metal sulfide colloidal quantum dot and said cations of said first shell are Cd^{2+}.

29. The nanoparticle of claim **24** wherein said quantum dot core is a metal sulfide colloidal quantum dot and said cations of said first shell are Cd^{2+} and said anions of said second shell are a member selected from the group consisting of halogen ions and thiocyanate ion.

30. The nanoparticle of claim **24** wherein said quantum dot core is a metal sulfide colloidal quantum dot, said cations of said first shell are Cd^{2+}, and said anions of said second shell are halogen ions.

31. The nanoparticle of claim **24** wherein said quantum dot core is a metal sulfide colloidal quantum dot, said cations of said first shell are Cd^{2+}, and said anions of said second shell are bromine ions.

32. A photoelectric device comprising:

a light-transmitting first electrode,

a first semiconductor layer in direct electrical contact with said first electrode,

a second semiconductor layer in direct electrical contact with said first semiconductor layer and comprising light-absorbing nanoparticles, each said nanoparticle comprising a quantum dot core, a first shell comprising cations that substantially completely surround said quantum dot core, and a second shell comprising anions that substantially completely surround said first shell, and

a second electrode in direct electrical contact with said second semiconductor layer.

33. The photoelectric device of claim **32** wherein said quantum dot core is a metal chalcogenide colloidal quantum dot.

34. The photoelectric device of claim **32** wherein said quantum dot core is a metal sulfide colloidal quantum dot.

35. The photoelectric device of claim **32** wherein said quantum dot core is a metal sulfide colloidal quantum dot and said cations of said first shell are a member selected from the group consisting of Cd^{2+}, Pb^{2+}, Zn^{2+}, and Sn^{2+}.

36. The photoelectric device of claim **32** wherein said quantum dot core is a metal sulfide colloidal quantum dot and said cations of said first shell are Cd^{2-}.

37. The photoelectric device of claim **32** wherein said cations of said first shell are Cd^{2+} and said anions of said second shell are a member selected from the group consisting of halogen ions and thiocyanate ion.

38. The photoelectric device of claim **32** wherein said quantum dot core is a metal sulfide colloidal quantum dot, said cations of said first shell are Cd^{2+}, and said anions of said second shell are halogen ions.

39. The photoelectric device of claim **32** wherein said quantum dot core is a metal sulfide colloidal quantum dot, said cations of said first shell are Cd^{2+}, and said anions of said second shell are bromine ions.

40. The photoelectric device of claim **32** wherein said first semiconductor layer is titanium dioxide.

41. The photoelectric device of claim **32** wherein said light-transmitting first electrode is a member selected from the group consisting of aluminum oxide, zinc oxide, indium tin oxide, and fluorine-doped tin oxide, and said second electrode is a member selected from the group consisting of nickel, lithium fluoride, platinum, palladium, silver, gold, copper, and alloys of silver, gold, and copper.

42. The photoelectric device of claim **32** wherein said light-transmitting first electrode is fluorine-doped tin oxide, and said second electrode is gold.

43. A method of forming passivated p-type semiconductor nanoparticles, said method comprising:

(a) treating p-type semiconductor colloidal quantum dots having surface anions with a solution of a cation-containing reagent that passivates said surface anions to form colloidal quantum dots coated with said cations, and

(b) treating said colloidal quantum dots so coated with a solution of an anion-containing reagent that passivates said cations.

44. The method of claim **43** said p-type semiconductor colloidal quantum dots are metal chalcogenide colloidal quantum dots.

45. The method of claim **43** said p-type semiconductor colloidal quantum dots are metal sulfide colloidal quantum dots.

46. The method of claim **43** said p-type semiconductor colloidal quantum dots are lead sulfide colloidal quantum dots.

47. The method of claim **43** said cation of said cation-containing reagent is a member selected from the group consisting of Cd^{2+}, Pb^{2-}, Zn^{2-}, and Sn^{2-}.

48. The method of claim **43** said cation of said cation-containing reagent is Cd^{2+}.

49. The method of claim **43** said anion of said anion-containing reagent is a member selected from the group consisting of halogen ions and thiocyanate ion.

50. The method of claim **43** said cation-containing reagent is cadmium(II) chloride-tetradecylphosphonic acid-oleylamine.

51. The method of claim **43** said anion of said anion-containing reagent is a member selected from the group consisting of halogen ions and thiocyanate ion.

52. The method of claim **43** said anion of said anion-containing reagent is a halogen ion.

53. The method of claim **43** said anion of said anion-containing reagent is a bromine ion

54. The method of claim **43** said anion-containing reagent is a member selected from the group consisting of cetyltrimethylammonium bromide, hexatrimethylammonium chloride, tetrabutylammonium iodide, and tetrabutylammonium thiocyanate.

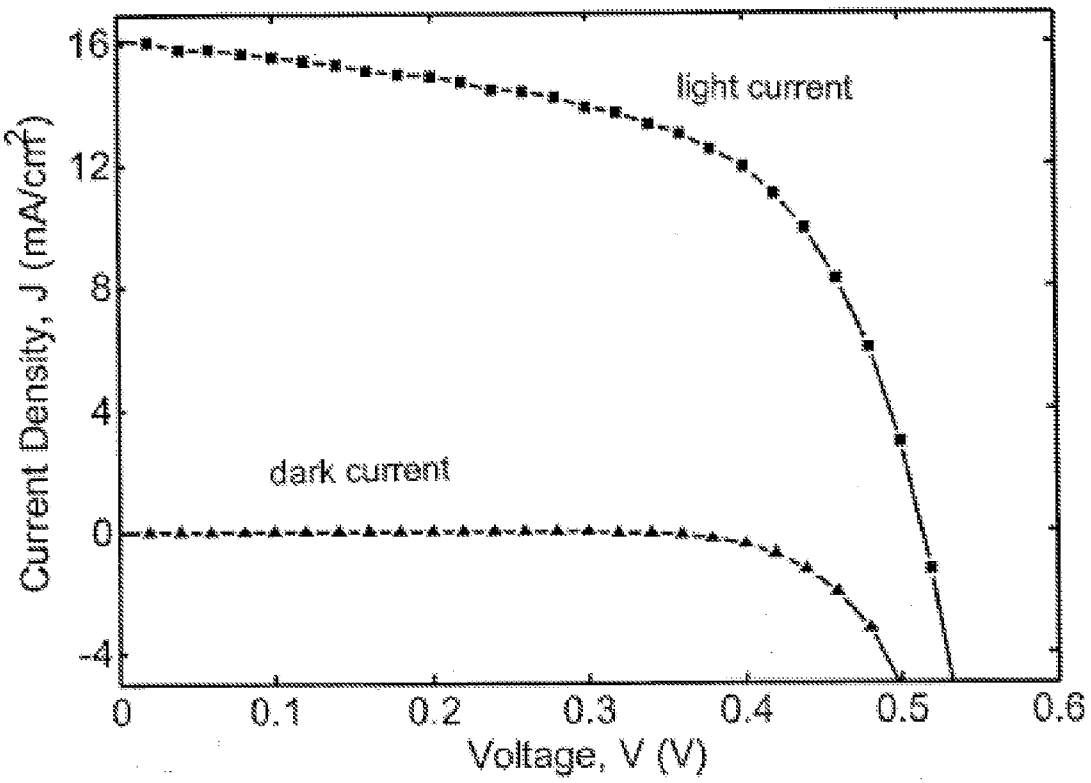
16
12
8
4
0
-4
Current Density, J (mA/cm2)
light current
dark current
0
0.1
0.2
0.3
0.4
0.5
0.6
Voltage, V (V)

FIG. 1

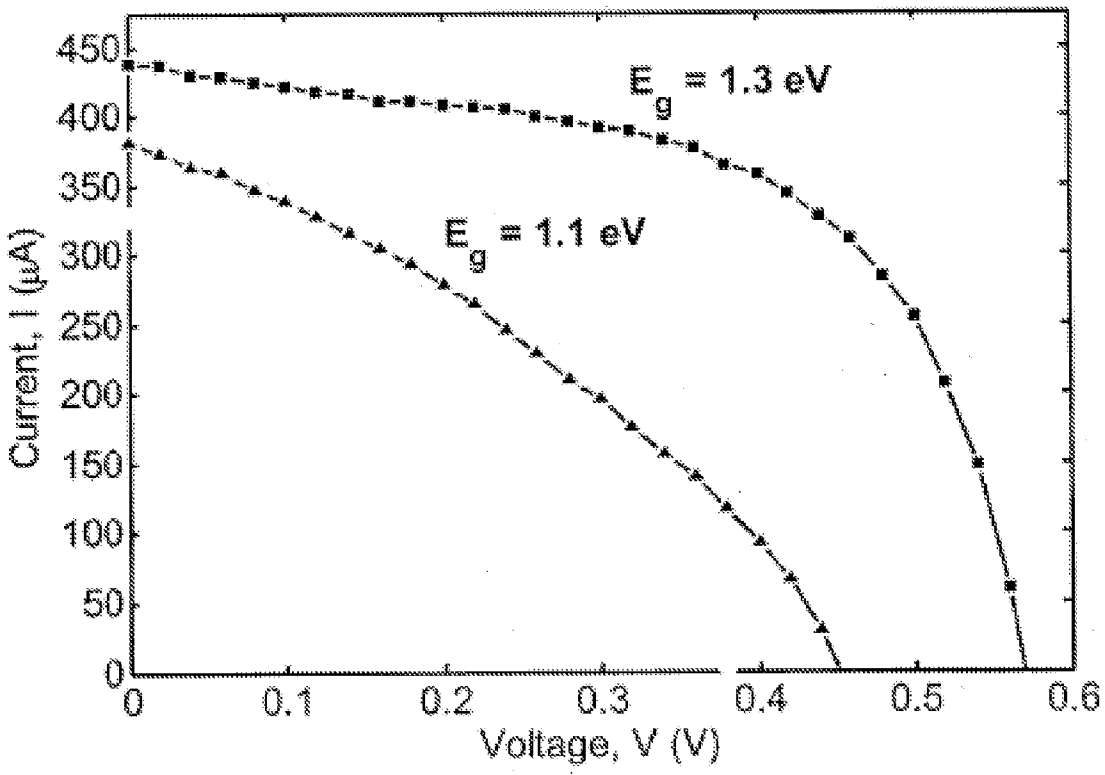
450
400
350
300
250
200
150
100
50
0
Current, I (μA)
0
0.1
0.2
0.3
0.4
0.5
0.6
Voltage, V (V)
E_g = 1.3 eV
E_g = 1.1 eV

FIG. 2

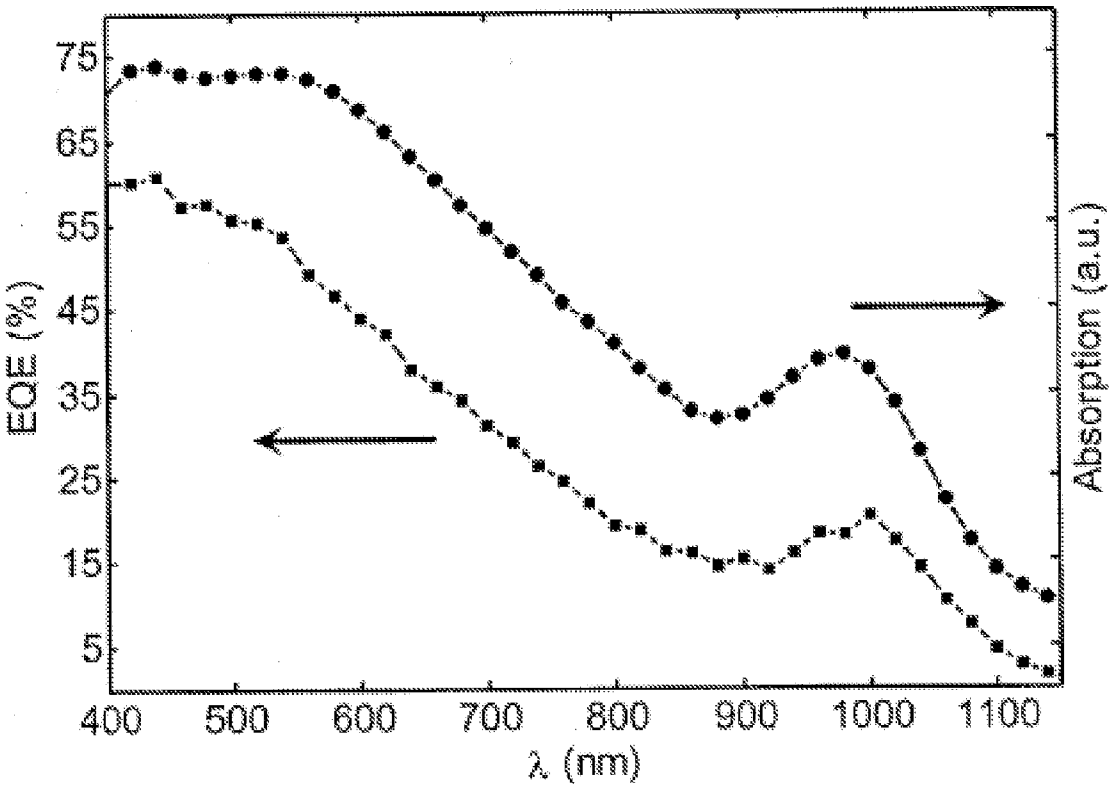
EQE (%)
75
65
55
45
35
25
15
5
400
500
600
700
800
900
1000
1100
λ (nm)
Absorption (a.u.)

FIG. 3

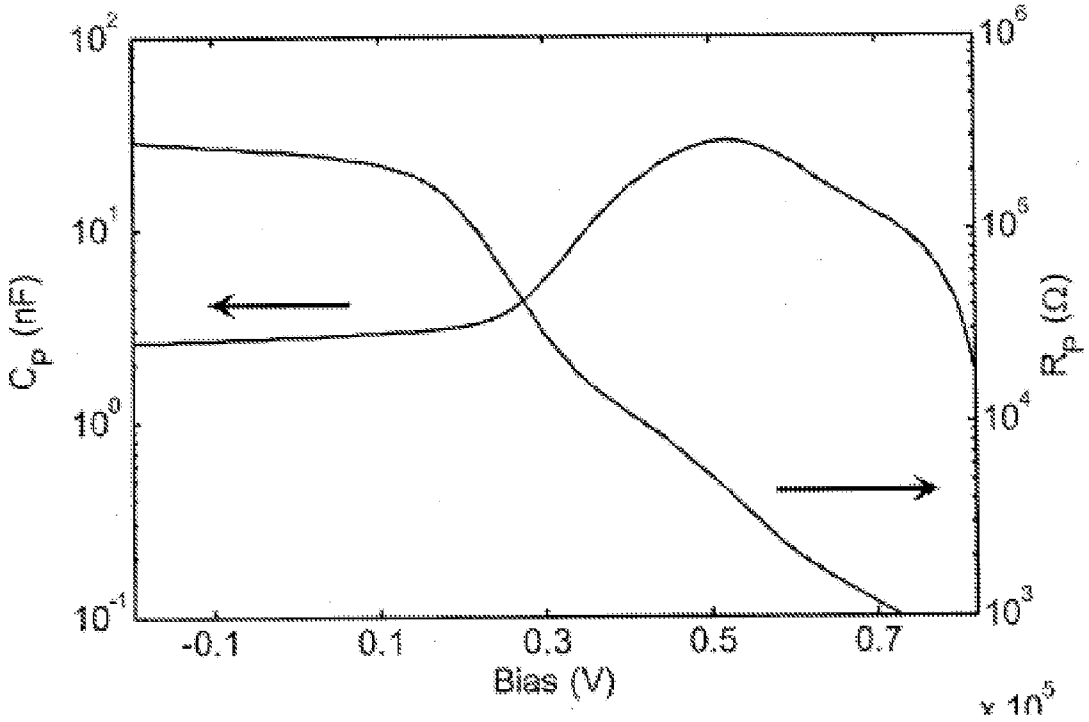
10^{2}
10^{1}
10^{0}
10^{-1}
C_p (nF)
10^{6}
10^{5}
10^{4}
10^{3}
R_p (Ω)
-0.1
0.1
0.3
0.5
0.7
Bias (V)
x 10^{5}

FIG. 4

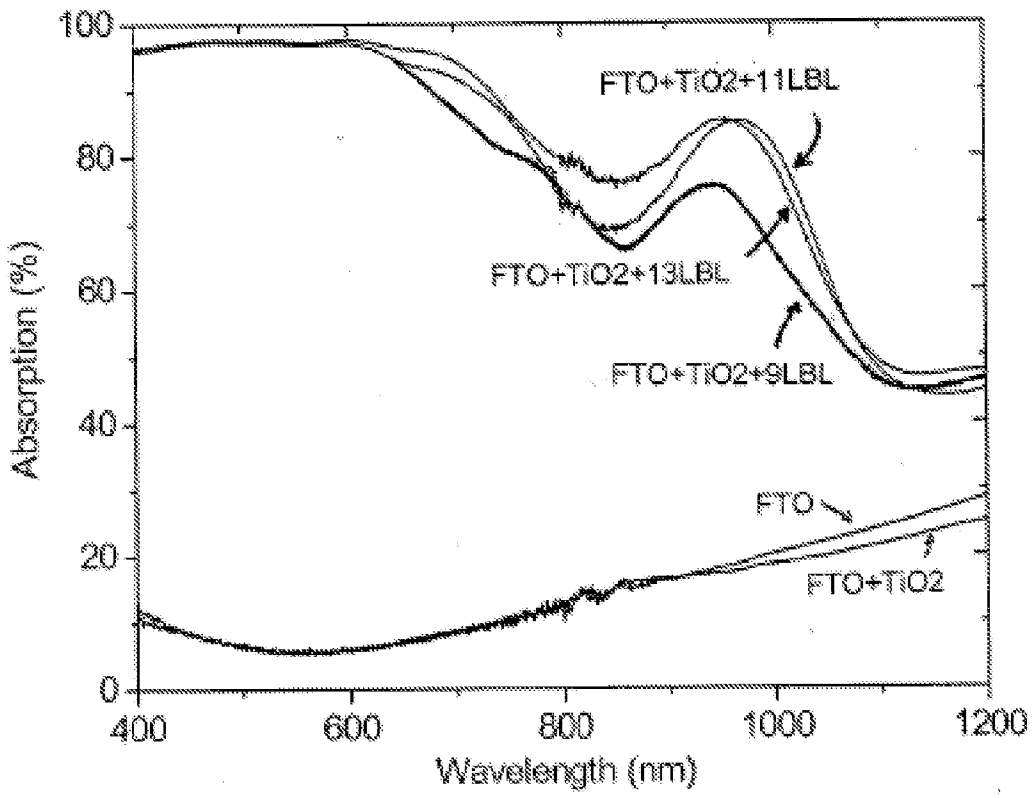
100
80
60
40
20
0
Absorption (%)
400
600
800
1000
1200
Wavelength (nm)
FTO+TiO2+11LBL
FTO+TiO2+13LBL
FTO+TiO2+9LBL
FTO
FTO+TiO2

FIG. 5

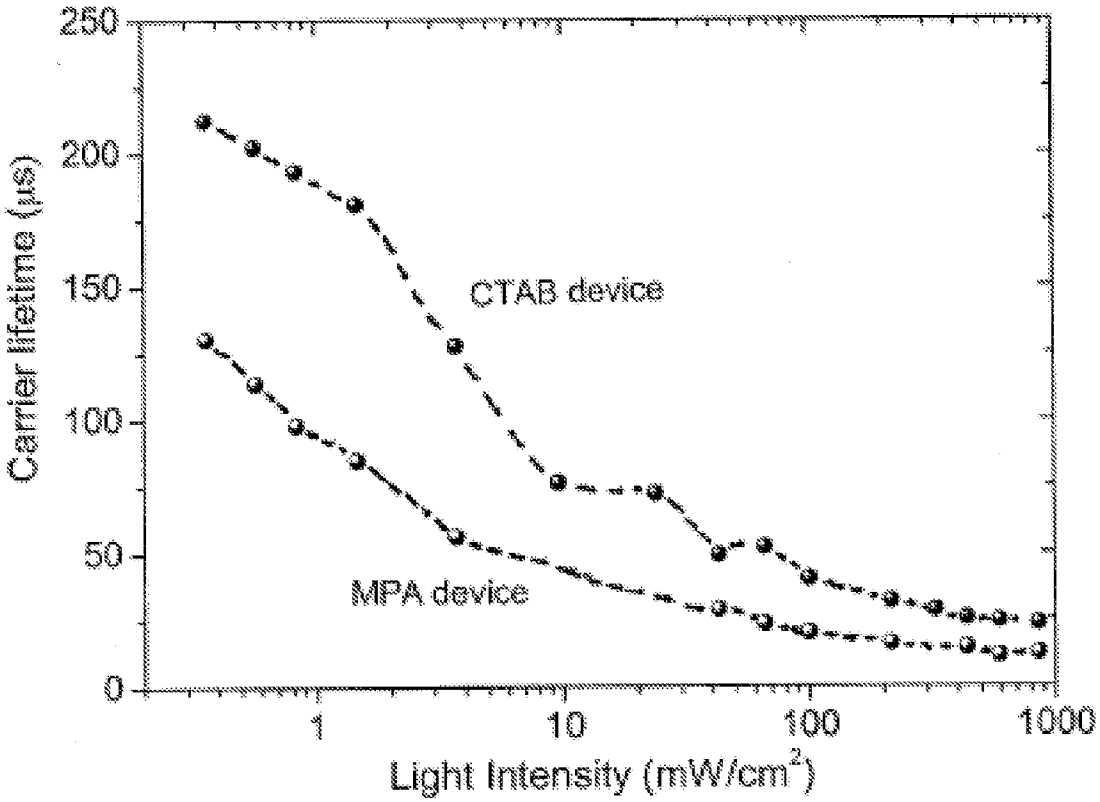
250
200
150
100
50
0
Carrier lifetime (μs)
CTAB device
MPA device
1
10
100
1000
Light Intensity (mW/cm2)

FIG. 6

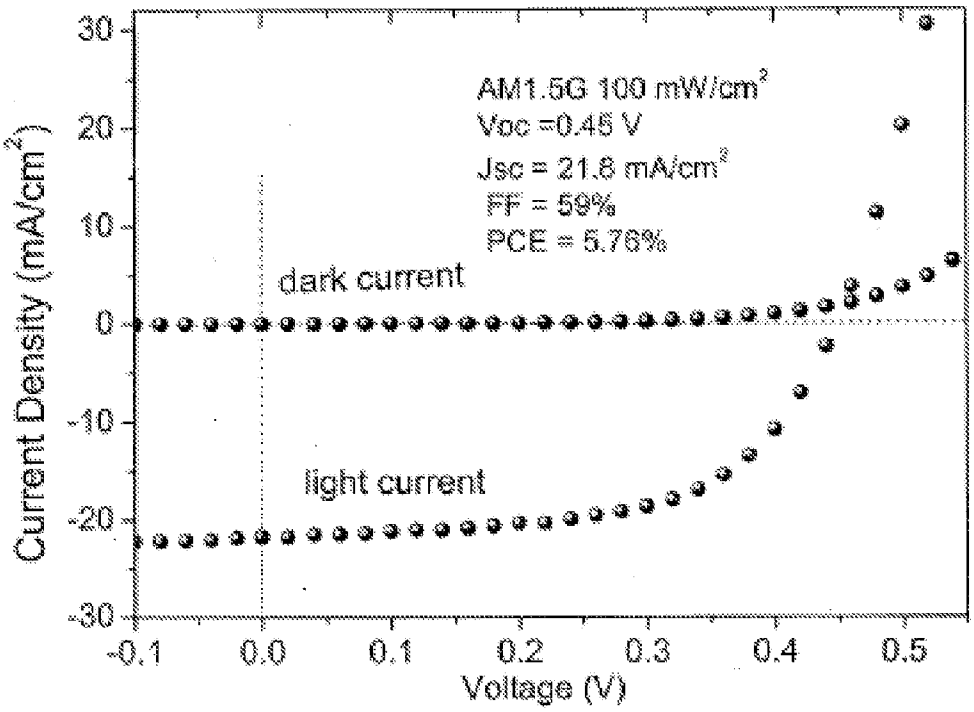
AM1.5G 100 mW/cm²
Voc =0.45 V
Jsc = 21.8 mA/cm²
FF = 59%
PCE = 5.76%
dark current
light current
Current Density (mA/cm²)
Voltage (V)
30
20
10
0
-10
-20
-30
-0.1
0.0
0.1
0.2
0.3
0.4
0.5

FIG. 7